Langmuir

Article

pubs.acs.org/Langmuir

Binding of Methylene Blue onto Langmuir Monolayers Representing Cell Membranes May Explain Its Efficiency as Photosensitizer in Photodynamic Therapy

Thaís F. Schmidt,[†] Luciano Caseli,[‡] Osvaldo N. Oliveira, Jr.,[§] and Rosangela Itri*[,∥]

[†]Federal University of ABC (UFABC), Santo André, SP 09210-580, Brazil

[‡]Institute of Environmental, Chemical, and Pharmaceutical Sciences, Federal University of São Paulo, Diadema, SP 09913-030, Brazil

[§]São Carlos Institute of Physics, University of São Paulo, São Carlos, SP 13560-970, Brazil

[∥]Institute of Physics, University of São Paulo, São Paulo, SP 05508-090, Brazil

ABSTRACT: We provide evidence for the electrostatic interactions between the cationic photosensitizer methylene blue (MB) and cell membrane models represented by neat and mixed Langmuir monolayers of dioleylphosphatidylcholine (DOPC) and 1,1′,2,2′-tetraoleoylcardiolipin (CL). From surface pressure measurements, MB was found to adsorb strongly and expand CL-containing monolayers, while it caused an apparent decreasing in molecular area on neat DOPC monolayer. The binding site of MB could be inferred from data with the surface-specific polarization-modulated infrared reflection−absorption spectroscopy (PM-IRRAS) technique, where changes induced by MB were observed in the vibrational modes of the phosphate groups of both CL and DOPC. The incorporation of MB also affected the carbonyl groups and the packing of the alkyl chains, thus indicating that MB binding site favors singlet oxygen generation close to the double bonds in the alkyl chains, an important requirement for photodynamic efficiency. Significantly, the data presented here demonstrate that MB may act in membranes composed by PCs, such as mammalian plasma membranes, and in those containing CL, as in bacterial and inner mitochondrial membranes.

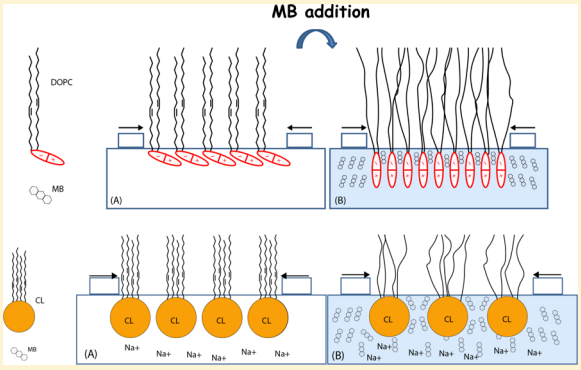

INTRODUCTION

Methylene blue (MB) is a cationic phenothiazine dye widely used in a variety of applications, including energy conversion,[1] histopathology staining, antimalarial therapy,[2] and the clinical treatment of methemoglobinaemia.[3] It is also a low-cost, water-soluble photosensitizer (PS) for neoplastic[4−6] and antimicrobial photodynamic therapy (PDT),[7−10] which exhibits lower toxicity to humans than to microbial cells, both in the dark and under illumination. PDT is mainly based on the photo-oxidation of lipid membranes,[11] where the PS absorbs light and generates reactive oxygen species (ROS), such as singlet oxygen that is considered the most powerful cytotoxic agent in PDT.[12] ROS are thus prone to promote oxidative reactions in the cell membrane, leading to molecular changes of unsaturated lipids. In its turn, the presence of oxidized lipids in the membrane may affect biophysical properties, e.g., membrane packing, permeability, and stretching modulus, eventually causing pore formation and membrane disruption.[13−15] ROS must be generated at a certain distance D in the aqueous solution surrounding the membrane due to their short lifetime (for instance, ∼3.5 μs for singlet oxygen in water[16] with $D \sim 100$ nm in model membranes[13]). In other words, PS must be located at distances smaller than D in the aqueous environment or into the lipid bilayer, allowing the encounter between the formed ROS and the double bonds of the alkyl chain in a photosensitization process.

The features that make MB important for PDT are as follows. MB absorbs light strongly in the region 630−680 nm, where visible light has a large penetration depth. It exhibits a high quantum yield of singlet oxygen production (on the order of 0.5) and has affinity to mitochondria,[17] which is relevant for a good PDT target because mitochondrial membrane damage triggers cell apoptosis. This affinity is probably related to electrostatic interactions between the positively charged MB and the inner mitochondria membrane which contains zwitterionic phosphatidylcholine (PC), phosphatidylethalonamine (PE), and negatively charged Cardiolipin (CL) (up to 9 mol %) lipids. CL is an unusual lipid with two phosphatidyl groups linked by a glycerol bridge (see Figure 1) and four acyl chains of varying lengths and degrees of unsaturation.[18,19] The presence of two phosphate groups may give rise to two negative charges. However, in aqueous dispersion at neutral pH, CL may contain a single charge only because one proton gets trapped in a bicyclic resonance structure formed by the two phosphates

Received: June 21, 2014
Revised: February 26, 2015
Published: March 23, 2015

DOI: 10.1021/acs.langmuir.5b00166
Langmuir 2015, 31, 4205−4212

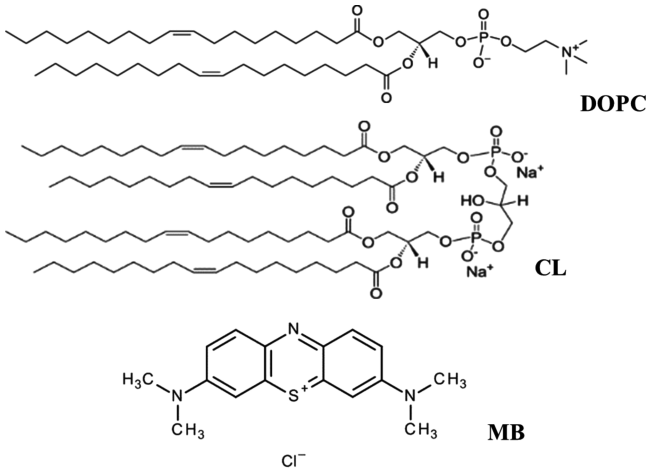

Figure 1. Chemical structures of 1,2-dioleoyl-*sn*-glycero-3-phosphocholine (DOPC), 1,1′,2,2′-tetraoleoylcardiolipin (CL), and methylene blue (MB).

and the central hydroxyl group.[19] Noteworthy, CL, PE, and the anionic lipid phosphatidylglycerol (PG) are the major components found in the membranes of several bacterial species.[20]

Therefore, unveiling the binding site of MB on PC and CL-containing membranes may help understanding and controlling the photo-oxidation mechanisms that underlie mitochondrial and bacterial membrane response to MB photodynamic action. In this study, we investigated the MB adsorption on neat and mixed Langmuir monolayers of dioleoyl-*sn*-glycero-3-phosphocholine (DOPC) and 1,1′,2,2′-tetraoleoylcardiolipin (CL). The so-called Langmuir monolayers are obtained by spreading amphiphilic molecules on the liquid−air interface and are accepted as a model for half a membrane.[21] Varying the DOPC:CL molar ratio allowed us to explore the role of the negatively charged phospholipid in MB−membrane interaction. Surface pressure and surface potential versus area isotherms permitted us to evaluate the MB binding and the changes induced in the in-plane elasticity. The MB binding site to CL and DOPC monolayers was also explored by polarization-modulation infrared reflection−absorption spectroscopy (PM-IRRAS),[22] which is a surface-specific spectroscopic technique able to identify not only the chemical groups at the interface but also the geometrical orientation of the related vibration dipole moments.[23] The use of PM-IRRAS was essential to unravel changes in the lipid polar head region at the air−aqueous solution interface and in the alkyl chains packing due to interaction between MB and DOPC and CL-containing lipid films.

MATERIALS AND METHODS

The Langmuir trough for obtaining surface pressure−area isotherms, adsorption kinetic curves, and PM-IRRAS measurements was a KSV minitrough with area dimensions of 365 mm × 75 mm. The surface tension was measured using a Wilhelmy plate. All measurements were carried out at 20 ± 1 °C with purified water (Milli-Q system, 18.2 MΩ cm and pH 6.3) in the absence and presence of 0.2 μM MB. Surface tension amounted to 72 mN/m, in good agreement with the value reported for pure water,[24] regardless of the presence of MB in the subphase. The MB concentration was chosen due to the predominance of MB monomers in the aqueous subphase rather than dimers/oligomers according to its electronic absorption spectrum (data not shown).

The lipids DOPC (1,2-dioleoyl-*sn*-glycero-3-phosphocholine) and CL (1′,3′-bis[1,2-dioleoyl-*sn*-glycero-3-phospho]-*sn*-glycerol (sodium salt)) were purchased from Avanti Polar Lipids with purity >99% and used without further purification. Methylene blue (MB) was acquired from Sigma-Aldrich (purity >90%) and used without purification. Figure 1 shows the chemical structures of the lipids and MB.

DOPC and CL solutions (1 mM) in chloroform were mixed at different molar ratios of 1:0, 0:1, 1:1, 1:2, and 2:1 and then spread on the subphase with the barrier fully opened. To evaluate the MB adsorption on the lipid monolayers, changes on the surface pressure were recorded up to 20 min of monolayer−MB solution contact. We continued the investigation by establishing a waiting time of 20 min between the spreading of the lipid on the MB subphase and the beginning of the surface pressure−area isotherms and PM-IRRAS experiments. This period of time was chosen to ensure the stability of the unsaturated lipid films that can be oxidized when exposed to the air for a long time.[25] The isotherms were obtained at a compression rate of 5 mm min^{-1}. Surface pressure and area were recorded simultaneously using the software provided by KSV. Based upon the volume deposited, lipid concentration, and the average molecular weight, the average area per lipid molecule was then calculated. The surface potential experiments were performed in a KSV Nima trough with volume of ca. 250 μL by using the vibrating capacitor method.[26]

PM-IRRAS measurements were performed using a KSV PMI 550 instrument by KSV Instruments. The Langmuir trough was set up so that the light beam reached the incidence monolayer at an angle of 80°. Such a value was chosen because it provided the best signal/noise ratio as well as the highest reflectivity. The spectrum—ranging from 4000 to 1000 cm^{-1}—was selected in different regions for better visualization of specific bands. This technique is highly sensitive and surface specific. The instrument, being positioned above the Langmuir trough, gets reflection−absorption information on the two fractions of the electrical component of the polarized light. PM-IRRAS takes advantage of the fact that p-polarized light (perpendicular to the reflective surface) is preferentially absorbed upon reflection, whereas s-polarized light is virtually unabsorbed. In contrast, absorption in isotropic media is independent of polarization, so that any difference between the s- and p-polarized signals can be assigned to surface specific absorption. The incoming light was continuously modulated between s- and p- polarization at a high frequency, which allowed simultaneous measurement of the spectra for the two polarizations. The difference thus provides surface specific information, and the sum gives the reference spectrum. As the spectra are measured simultaneously, the effect of water vapor can be largely reduced,[27,28] which is explained by the surface selection rule for PM-IRRAS.[29] For incidence angles above the Brewster angle, positive bands suggest dipole moment orientation parallel to the air−water interface while negative bands indicate dipole moment orientation perpendicular to the interface.[28,30]

RESULTS AND DISCUSSION

The interaction of MB with CL-containing monolayers at zero surface pressure promoted an increase in surface pressure with time, as shown in Figure 2. The effect was more pronounced for increasing CL concentration in the DOPC:CL mixed monolayers. The adsorption of the positively charged MB may be attributed to electrostatic attraction to the CL monolayer, which is believed to be negatively charged according to molecular dynamics simulation results on CL-containing bilayers, where 68% of the sodium counterions were not bound to CLs.[31] In contrast to CL-containing monolayers, Figure 2 shows no effect from MB on a pure DOPC monolayer, which may indicate a distinct adsorption mechanism of MB to lipids with zwitterionic polar head. Indeed, this lack of change in surface pressure could be indicative of absence of interaction, which is not the case as we shall see when discussing surface potential and PM-IRRAS measurements later on in the paper.

DOI: 10.1021/acs.langmuir.5b00166
Langmuir 2015, 31, 4205−4212

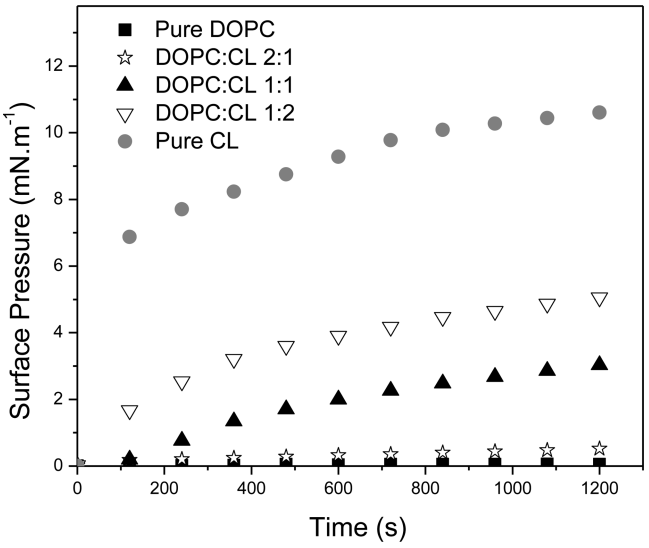

Figure 2. Time evolution of surface pressure of DOPC:CL monolayers dispersed in aqueous solution containing 0.2 μM MB. Lipid molar ratios are indicated in the figure.

The effect from incorporating MB in the surface pressure isotherms was investigated with the monolayers in the absence of MB in the subphase and with MB after 20 min of adsorption to avoid any lipid chain oxidation. Figure 3A shows the surface pressure−area isotherms for monolayers of DOPC, CL, and DOPC:CL at the molar ratio 2:1, whereas Figure 3B displays the corresponding in-plane elasticity isotherms. For the monolayers of neat compounds, the area per CL molecule is nearly twice the area occupied by DOPC at any surface pressure, as expected from the distinct chemical structures comprising four acyl chains for CL and two for DOPC (Figure 1). In particular, at π = 30 mN/m (considered as membrane pressure) values of DOPC and CL molecular areas correspond to 60 and 110 Å^2, respectively (Figure 3A), in good agreement with values reported in the literature.[32,33]

The average area per molecule for an ideal mixed monolayer with two components can be calculated from $A_{ij} = (x_iA_i + x_jA_j)$, where A_i and x_i are the molecular area and the mole fraction of each component at the same surface pressure, respectively.[34,35] Experimentally measured areas for mixed monolayers larger than A_{ij} indicate that repulsive forces act between the distinct components, whereas measured areas smaller than A_{ij} indicate attractive forces between the two components.[36] The DOPC:CL 2:1 mixed monolayer (as well as for DOPC:CL 1:1 and 1:2 molar ratios, whose data are not shown) exhibited larger average molecular areas than that predicted from the additive rule at all surface pressures. Such finding suggests the formation of a heterogeneous mixed lipid film due to repulsive interaction between CL and DOPC. This behavior contrasts with previous experimental results for PC−CL mixed monolayers,[36] although dynamic simulation on CL−PC mixed bilayers indicates the formation of CL aggregates dispersed in the PC membrane.[31] Brewster angle and fluorescence microscopy images (not shown) did not reveal any macrodomain formation or phase separation at the surface pressures studied.

The compressional modulus, C_s^{-1}, was calculated from the surface pressure isotherms as $-A(\partial\pi/\partial A)_T$, where A and π are the molecular area and the surface pressure, respectively, at a given temperature. Upon compression of the CL monolayer,

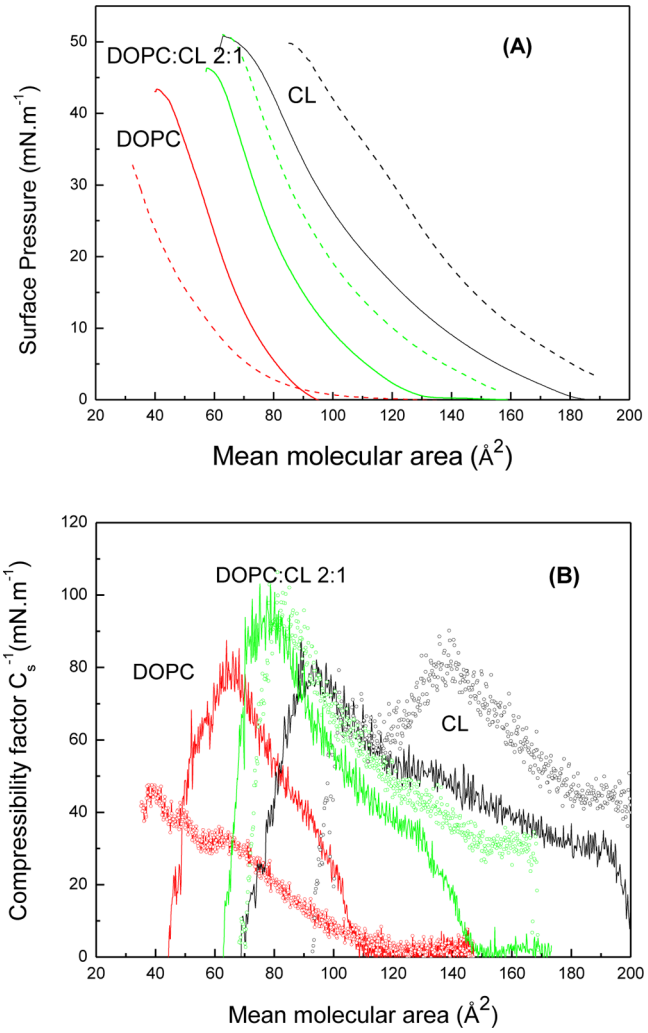

Figure 3. (A) Surface pressure−area isotherms of DOPC (red color), CL (black color), and DOPC:CL 2:1 (green color) monolayers at the air−water interface in the absence (solid lines) and presence of 0.2 μM MB (open symbols) after 20 min of adsorption. (B) Corresponding curves for the compressional modulus.

C_s^{-1} increased to reach a maximum around 80 mN m^{-1} at 95 Å^2, decreasing afterward (Figure 3B). For DOPC, C_s^{-1} also increased under compression, reaching 80 mN m^{-1} at 65 Å^2 per molecule (Figure 3B). This maximum elastic modulus value is of the order of that previously reported for monolayers of PC and CL.[36]

Focusing now on the effect from MB adsorption, we note from Figure 3A that MB caused significant expansion of CL monolayer, consistent with the results on adsorption with strong MB−CL interaction and with the literature.[37] The same applies to the mixed DOPC:CL (2:1 molar ratio) monolayer, for which MB caused expansion. In contrast, for the neat DOPC monolayer the incorporation of MB led to an apparent condensation of the monolayer, with a smaller area per molecule. This result obviously needs to be analyzed with caution because lowering of the area occupied per DOPC molecule would be unlikely. Also, distinctively different was the behavior of C_s^{-1}, since for DOPC it decreased significantly owing to the presence of MB, as indicated in Figure 3B. One should contrast with the MB effect on the other monolayers, where there was practically only a shift in area per molecule for

DOI: 10.1021/acs.langmuir.5b00166
Langmuir 2015, 31, 4205−4212

the C_s^{-1} dependence, whereas the maximum value in each curve was not altered significantly. Therefore, the surface pressure and elasticity data do not suffice to provide a model for the adsorption of MB on the zwitterionic DOPC monolayer, which is one of the reasons we had to resort to a spectroscopic method, as discussed later.

The surface potential isotherms in Figure 4 show significant reduction of the potential for DOPC monolayer interacting

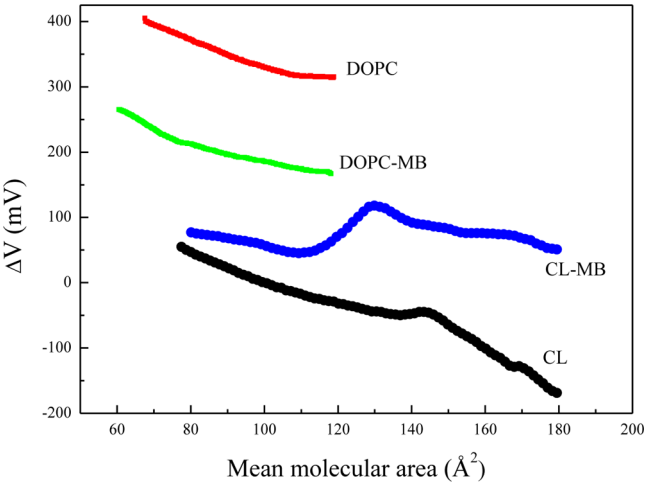

Figure 4. Surface potential for DOPC and CL monolayers at air–water interface and under MB influence in an elapsed time of 20 min.

with MB, probably due to solvation of polar heads by MB molecules. In the case of CL monolayer in contact with MB under compression, an increase in potential was observed, thus reaching a maximum value when the mean molecular area was ca. 130 Å^2. This behavior parallels to that observed for C_s^{-1} values (Figure 3B) due to the lipid packing followed by molecular rearrangement afterward. Furthermore, the interaction of MB with CL headgroup charges is such that it tends to neutralize the potential of the electrical double layer (which is negative), then causing the measured surface potential to increase.

The coupling of MB onto the lipid monolayers was assessed by taking PM-IRRAS spectra after 20 min of MB adsorption in DOPC and CL monolayers, from which information can be inferred on the vibration moment of some chemical groups oriented at the interface. The effect of MB is remarkable for both monolayers. For DOPC, Figure 5 indicates that MB affects the headgroup as well as the alkyl chains. The bands assigned to the phosphate group can be appreciated in the 1050–1300 cm^{-1} region.[38,39] For DOPC monolayer in contact with aqueous subphase without MB, asymmetric and symmetric P═O stretching vibration modes are observed at 1265 cm^{-1} ($\nu_{as}(PO_2^-)$) and 1128 cm^{-1} ($\nu_{sim}(PO_2^-)$), respectively, whereas the asymmetric single bond C–O stretch of the ester phosphate group ν(C–O[P]) is appreciated at 1070 cm^{-1} (Figure 5A1). In the presence of MB, the $\nu_{as}(PO_2^-)$ and $\nu_{sim}(PO_2^-)$ are displaced to 1269 and 1144 cm^{-1}, respectively, and had their direction inverted. This means that the orientation of this group was altered due to MB interaction. Further, the signal of ν(C–O[P]) practically disappeared (Figure 5A2). On the other hand, a peak centered at 1168 cm^{-1} appears in the spectra (Figure 5A2) probably due to the stretching mode of NCH_3 group of MB[40] that is disposed in the aqueous–monolayer film interface.

The PM-IRRAS signal of the carbonyl ester group stretch ν(C═O) of a phospholipid molecule can be appreciated in the 1800–1600 cm^{-1} region.[38,39] For the case of a neat DOPC monolayer two bands, one centered at 1717 cm^{-1} and the other one centered at 1774 cm^{-1} (Figure 5B1), are observed, corresponding to hydrated and nonhydrated carbonyl ester groups vibration,[38] respectively. Some bands between 1600 and 1700 cm^{-1} appear in the spectra as result of the difference in reflectivity of the water interface covered with the monolayer and that not covered with the monolayer. Upon MB influence, the nonhydrated ν(C═O) is displaced to 1743 ± 2 cm^{-1} (Figure 5B2), whereas a less defined peak of the hydrated ν(C═O) takes place at 1717 cm^{-1} and had its intensity significantly diminished. Such observations may be associated with changes in the solvation of the carbonyl group. Therefore, MB affects hydration nearby DOPC headgroups, probably being located near the phosphate and carbonyl groups of the DOPC, similarly to what has been observed for some monovalent ions.[41]

Figures 5C1 and 5C2 show the bands assigned to CH_2 and CH_3 stretching in the hydrophobic tails between 2950 and 2750 cm^{-1}.[38,39,42] The band centered at 2915 cm^{-1} is attributed to antisymmetric stretches of CH_2, and the one at 2866 cm^{-1} is attributed to symmetric stretches. The bands at 2895 and 2810 cm^{-1} are attributed to CH stretches in CH_3. When MB is incorporated, these bands become less defined, which is associated with loss of order in the monolayer induced by MB, with the tails squirming each other. For lipids with unsaturation in the hydrophobic moieties, such as DOPC, the tails can disturb the neighboring molecule.

On the basis of the results from isotherms and PM-IRRAS, we propose a schematic model depicted in Figure 6 for the arrangement of DOPC molecules in the Langmuir monolayer, where the negative and positive signs represent the phosphate and choline groups, respectively. For a neat DOPC monolayer, the electric dipole moment of the zwitterionic phosphatidylcholine head is assumed to be oriented almost parallel to the air–water interface, as indicated in Figure 6A, following the work of Barbosa et al.[43] The binding of the cationic MB is then governed by ion-dipole interaction in such a way that the positively charged cationic molecule tends to be near the phosphate headgroup. Upon interacting with MB, our results suggest the polar heads of DOPC (and hence the dipole moments) change orientation as illustrated in Figure 6B, which explains the inversion in the direction of the phosphate bands in Figures 5A1 and 5A2. The tilting in the zwitterion induced by MB should lead to a decrease in the normal component of the dipole moment and consequently a decrease in surface potential, as was indeed observed experimentally in Figure 4. Moreover, the approximation of polar heads in such a configuration yields smaller areas per molecule, consistent with the surface pressure isotherms in Figure 3. Incidentally, this decrease in area induced by MB explains why no change in surface pressure was observed in the adsorption kinetics experiments in Figure 2. Since the headgroups will be deeper into the water subphase (cf. Figure 6B), the intensity of ν(C–O[P]) disappears. Also closer to the subphase will be the C═O groups, thus explaining the changes induced by MB in Figure 5B2 which were ascribed to solvation. Finally, the displacement of the lipids deeper toward the subphase promotes the disorder of the alkyl chains (Figure 6B) due to lateral friction between them, consistent with the changes in the CH_2 and CH stretches signals in the PM-IRRAS spectra of Figure 5C.

DOI: 10.1021/acs.langmuir.5b00166
Langmuir 2015, 31, 4205–4212

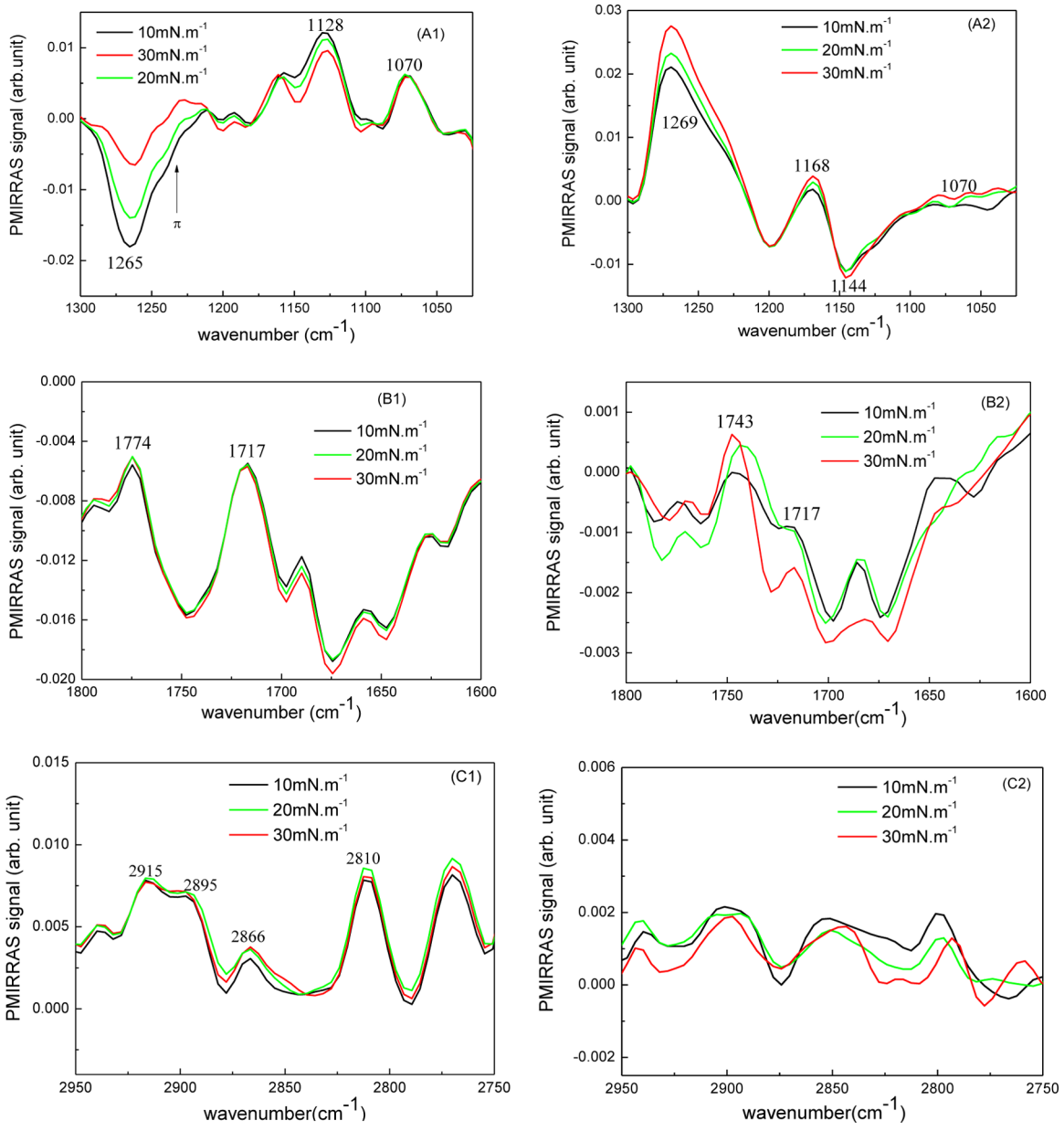

Figure 5. PM-IRRAS spectra for DOPC monolayers at the air−water interface (left) and after 20 min of MB adsorption (right): (A) phosphate group; (B) carbonyl group; (C) CH_3 and CH_2 groups. See text for details.

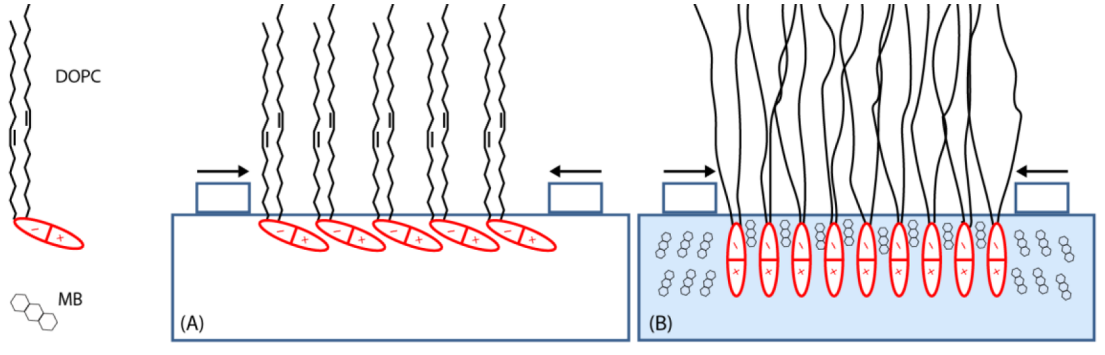

Figure 6. Proposed model for DOPC−MB interaction: (A) DOPC monolayer at air−water interface; (B) under MB influence. The unsaturations in the disordered alkyl chains were omitted in (B) for clarity.

For CL monolayers, the PM-IRRAS spectra area displayed in Figure 7. The band centered in 1269 cm^{-1}, attributed to the ($\nu_{as}(PO_2^-)$ stretch, is more defined with CL compression (Figure 7A1). On the other hand, the bands at 1163 and 1070

DOI: 10.1021/acs.langmuir.5b00166
Langmuir 2015, 31, 4205−4212

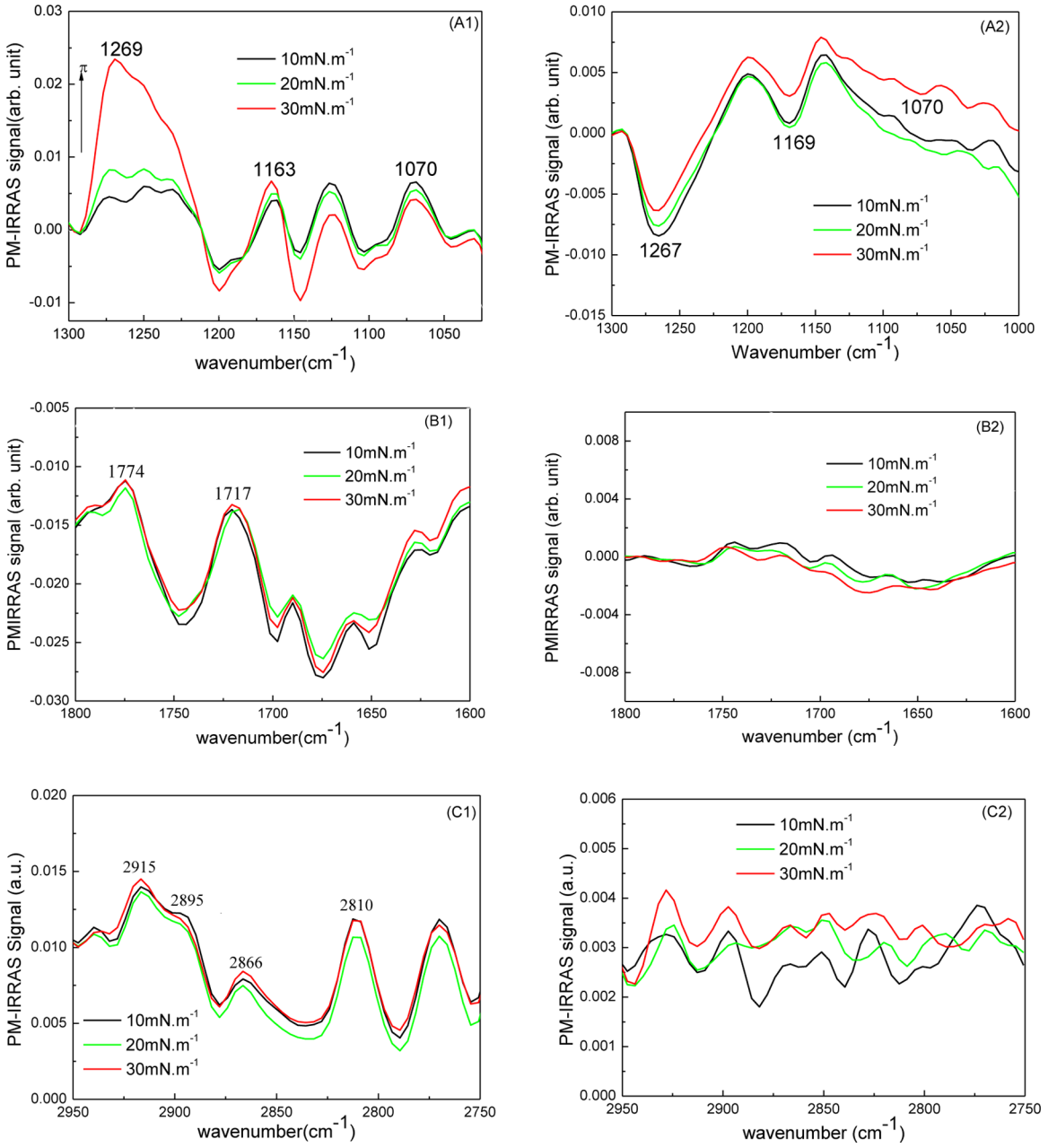

Figure 7. PM-IRRAS spectra for CL monolayers at air−water interface (left) and under MB influence after 20 min MB adsorption (right): (A) phosphate group; (B) carbonyl group; (C) CH_3 and CH_2 groups. See text for details.

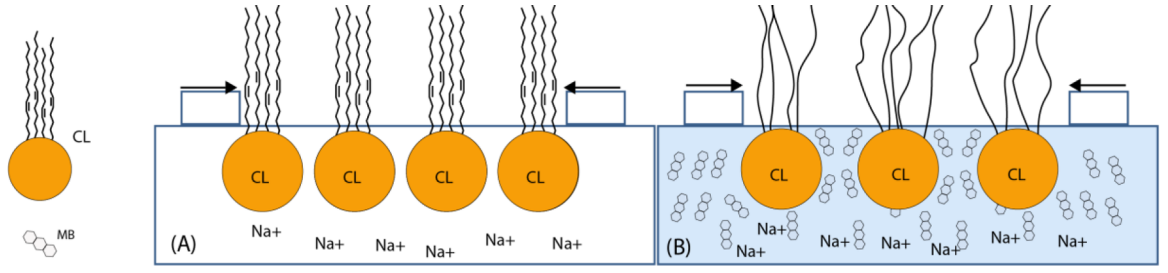

Figure 8. Proposed model for CL−MB interaction: (A) CL monolayer at air−water interface; (B) under MB influence. The unsaturations in the disordered alkyl chains were omitted in (B) for clarity.

cm^{-1} associated with $\nu_{sim}(PO_2^-)$ and ν(C−O[P]) stretches (Figure 7A1), respectively, are not altered by compression. Of note, the orientation of the phosphate groups is altered by interaction with MB, as the direction of the bands is inverted with small position displacements (Figure 7A2). The single bond C−O stretch from the C−O[P] group loses it signal upon

DOI: 10.1021/acs.langmuir.5b00166
Langmuir 2015, 31, 4205−4212

MB influence (Figure 7A2), similarly to what was observed for DOPC monolayer (Figure 5A2). The incorporation of MB also causes a drastic loss of definition of the C═O bands (Figure 7B2), in sharp contrast to the effects induced in DOPC monolayers (Figure 5B2). Without MB, the bands are centered at 1774 and 1716 cm^{-1} (Figure 7B1) corresponding to carbonyl stretches for nonhydrated and hydrated groups, respectively. With MB incorporation, it is clear that these bands lose definition, which indicates loss of order of these groups caused by the interaction between MB and CL. Figure 7C1 shows the bands in 2915 and 2866 cm^{-1} that are attributed to CH_2 stretches for antisymmetric and symmetric vibration modes, respectively. The bands at 2895 and 2810 cm^{-1} are attributed to CH stretches in CH_3 groups. Therefore, with MB in the monolayer, the IR signals of CH_2 and CH stretches are less defined which may be attributed to chain disorder.

The model proposed for the interaction between the positively charged MB and the negatively charged CL monolayer is depicted in Figure 8, being consistent with the whole data presented here. The strong electrostatic attraction leads to MB molecules permeating the entire region of the CL polar heads, thus causing increase in pressure in the kinetics experiments (Figure 2) and expansion in the surface pressure isotherms (Figure 3). Furthermore, adsorption of MB should decrease the negative contribution of the double layer to the surface potential in a CL monolayer, which results in an increased surface potential, as observed in Figure 4. The phosphate and carbonyl groups would be affected by MB, as denoted in the large changes in the PM-IRRAS spectra of Figures 7A and 7B. The model in Figure 8 also predicts considerable chain disorder induced by MB, consistent with the loss of definition of the CH_2 and CH_3 bands due to the hydrophobic chains in Figure 7C2.

■ CONCLUSIONS

The use of Langmuir monolayers as a simplified model membrane coupled to PM-IRRAS results allowed us to propose a mechanism for the electrostatically driven interactions between the photosensitizer MB and DOPC and CL phospholipid monolayers. Although MB is a water-soluble photosensitizer, the adsorption measurements clearly showed that it adsorbs at the charged lipid-containing monolayers, as evidenced by both changes in surface pressure and surface potential isotherms. This corroborates the reported MB efficiency on antimicrobial phototherapy,[7−10] since MB effectively binds to negatively charged membranes. The mechanism of MB interaction with the polar head groups of DOPC and CL via electrostatic interaction, depicted in Figures 6 and 8, respectively, is such that it allows for its adsorption up to the carbonyl groups of the lipid molecules. As a consequence, the MB binding near the double bonds of the alkyl chains may favor the lipid oxidation via singlet oxygen photogeneration in membranes composed mainly of PC, such as mammalian plasma membranes, and in those containing CL, as in the bacterial and inner mitochondrial membranes. An excess of lipid chemical modifications conducts to membrane damage,[12−15] eventually leading to cell death.

■ AUTHOR INFORMATION

Corresponding Author

*(R.I.) Phone (55-11-30917012); e-mail itri@if.usp.br.

Notes

The authors declare no competing financial interest.

■ ACKNOWLEDGMENTS

This work was supported by grant #2012/50680-5, São Paulo Research Foundation (FAPESP), and nBioNet from CAPES. T.F.S. was a recipient of an FAPESP PhD fellowship (process: 2008/07240-9). The authors thank Maurício S. Baptista and Luis Gustavo Dias for valuable discussions. R.I., L.C., and O.N.O.J. also acknowledge CNPq for research fellowships.

■ REFERENCES

(1) Chan, M. S.; Bolton, J. R. Structures, Reduction Potential and Absorption Maxima of Synthetic Dyes of Interest in Photochemical Solar Energy Storage Studies. *Sol. Energy* **1980**, *24*, 561−574.

(2) Wainwright, M.; Crossley, K. B. Methylene Blue − A Therapeutic Dye for All Seasons? *J. Chemother.* **2002**, *14*, 431−443.

(3) Wright, R. O.; Lewander, W. J.; Woolf, A. D. Methemoglobinemia: Etiology, Pharmacology, and Clinical Management. *Ann. Emerg. Med.* **1999**, *34*, 646−656.

(4) Orth, K.; Beck, G.; Genze, F.; Ruck, A. Methylene Blue Mediated Photodynamic Therapy in Experimental Colorectal Tumors in Mice. *J. Photochem. Photobiol., B* **2000**, *57*, 186−190.

(5) Tardivo, J. P.; Del Giglio, A.; Paschoal, L. H.; Baptista, M. S. New Photodynamic Therapy Protocol to Treat Aids-Related Kaposi's Sarcoma. *Photomed. Laser Surg.* **2006**, *24*, 528−531.

(6) Wagner, M.; Suarez, E. R.; Theodoro, T. R.; Machado, C. D. A. S.; Gama, M. F. M.; Tardivo, J. P.; Paschoal, F. M.; Pinhal, M. A. S. Methylene Blue Photodynamic Therapy in Malignant Melanoma Decreases Expression of Proliferating Cell Nuclear Antigen and Heparanases. *Clin. Exp. Dermatol.* **2012**, *37*, 527−533.

(7) Wainwright, M.; Phoenix, D. A.; Gaskell, M.; Marshall, B. Photobactericidal Activity of Methylene Blue Derivatives Against Vancomycin-Resistant *Enterococcus* spp. *J. Antimicrob. Chemother.* **1999**, *44*, 823−825.

(8) Tardivo, J. P.; Wainwright, M.; Baptista, M. S. Local Clinical Phototreatment of Herpes Infection in São Paulo. *Photodiag. Photodyn. Ther.* **2012**, *9*, 118−121.

(9) Scwingel, A. R.; Barcessat, A. R. P.; Núñez, S. C.; Ribeiro, M. S. Antimicrobial Photodynamic Therapy in the Treatment of Oral Candidiasis in HIV-Infected Patients. *Photomed. Laser Surg.* **2012**, *30* (8), 429−432.

(10) Yolanda, G.; Carmen, A.; Carmen, A. M.; Elena, A.-C.; Blanca, F.; Revillo, M. J.; Hamblin, M. R.; Rezusta, A. Cutaneous Sporotrichosis Treated with Photodynamic Therapy: An *In Vitro* and *In Vivo* Study. *Photomed. Laser Surg.* **2014**, *32* (1), 54−57.

(11) Thorpe, W. P.; Toner, M.; Ezzell, R. M.; Tompkins, R. G.; Yarmush, M. L. Dynamics of Photoinduced Cell Plasma Membrane Injury. *Biophys. J.* **1995**, *68*, 2198−2206.

(12) Itri, R.; Junqueira, H. C.; Mertins, O.; Baptista, M. S. Membrane Changes Under Oxidative Stress: the Impact of Oxidized Lipids. *Biophys. Rev.* **2014**, *6*, 47−61.

(13) Caetano, W.; Haddad, P. S.; Itri, R.; Severino, D.; Vieira, V. C.; Baptista, M. S.; Schroder, A.; Marques, C. Photo-Induced Destruction of Giant Vesicles in Methylene Blue Solutions. *Langmuir* **2007**, *23*, 1307−1314.

(14) Cwiklik, L.; Jungwirth, P. Massive Oxidation of Phospholipid Membranes Leads to Pore Creation and Bilayer Disintegration. *Chem. Phys. Lett.* **2010**, *48*, 99−103.

(15) Mertins, O.; Bacellar, I. O. L.; Thalmann, F.; Marques, C. M.; Baptista, M.; Itri, R. Physical Damage on Giant Vesicles Membrane as a Result of Methylene Blue Photoirradiation. *Biophys. J.* **2014**, *106*, 162−171.

(16) Wilkinson, F.; Helman, W. P.; Ross, A. B. Rate Constants for the Decay and Reactions of the Lowest Electronically Excited Singlet-State of Molecular-Oxygen in Solution − An Expanded and Revised Compilation. *J. Phys. Chem. Ref. Data* **1995**, *24*, 663−1021.

DOI: 10.1021/acs.langmuir.5b00166
Langmuir 2015, 31, 4205−4212

(17) Gabrielli, D.; Belisle, E.; Baptista, M. S. Binding, Aggregation and Photochemical Properties of Methylene Blue in Mitochondrial Suspensions. *Photochem. Photobiol.* **2004**, *79*, 227−232.
(18) Schlame, M.; Ren, M.; Xu, Y.; Greenberg, M. L.; Haller, Y. Molecular Symmetry in Mitochondrial Cardiolipins. *Chem. Phys. Lipids* **2005**, *138*, 38−49.
(19) Schlame, M. Cardiolipin Synthesis for the Assembly of Bacterial and Mitochondrial Membranes. *J. Lipid Res.* **2008**, *49*, 1607−1620.
(20) Epand, R. F.; Pollard, J. E.; Wright, J. O.; Savage, P. B.; Epand, R. M. Depolarization, Bacterial Membrane Composition, and the Antimicrobial Action of Ceragenins. *Antimicrob. Agents Chemother.* **2010**, *54*, 3708−3713.
(21) Brockman, H. Lipid Monolayers: Why Use Half a Membrane to Characterize Protein-Membrane Interactions? *Curr. Opin. Struct. Biol.* **1999**, *9*, 438−444.
(22) Buffeteau, T.; Desbat, B.; Turlet, J. M. Polarization Modulation FT-IR Spectroscopy of Surfaces and Ultra-Thin Films: Experimental Procedure and Quantitative Analysis. *Appl. Spectrosc.* **1991**, *45*, 380−389.
(23) Mendelshon, R.; Mao, G.; Flach, C. R. Infrared Reflection−Absorption Spectroscopy: Principles and Applications to Lipid−Protein Interaction in Langmuir Films. *Biochim. Biophys. Acta* **2010**, *1798*, 788−800.
(24) Vargaftik, N. B.; Volkov, B. N.; Voljak, L. D. International Tables of the Surface Pressure of Water. *J. Phys. Chem. Ref. Data* **1983**, *12*, 817−820.
(25) Liljeblad, J. F. D.; Bulone, V.; Tyrode, E.; Rutland, M. W.; Magnus Johnson, C. Phospholipid Monolayers Probed by Vibrational Sum Frequency Spectroscopy: Instability of Unsaturated Phospholipids. *Biophys. J.* **2010**, *98*, L50−L52.
(26) Yamins, H. G.; Zisman, W. A. A New Method of Studying the Electrical Properties of Monomolecular Films on Liquids. *J. Chem. Phys.* **1933**, *1*, 656−661.
(27) Dicko, A.; Bourque, H.; Pézolet, M. Study by Infrared Spectroscopy of the Conformation of Dipalmitoylphosphatidylglyrecol Monolayers at the Air-Water Interface and Transferred on Solid Substrates. *Chem. Phys. Lipids* **1998**, *96*, 125−139.
(28) Blaudez, D.; Turlet, J. M.; Dufourcq, J.; Bard, D.; Buffeteau, T.; Desbat, B. Investigations at the Air/Water Interface Using Polarization Modulation IR Spectroscopy. *J. Chem. Soc., Faraday Trans.* **1996**, *92*, 525−530.
(29) Urakawa, A.; Bürgi, T.; Baiker, A. Modulation Excitation PM-IRRAS: A New Possibility for Simultaneous Monitoring of Surface and Gas Species and Surface Properties. *Chimia* **2006**, *60*, 231−233.
(30) Vié, V.; Legardinier, S.; Chieze, L.; Le Bihan, O.; Oin, Y.; Sarkis, J.; Hubert, J. F.; Renault, A.; Desbat, B.; Le Rumeur, E. Specific Anchoring Modes of Two Distinct Dystrophin Rod Sub-Domains Interacting in Phospholipid Langmuir Films Studied by Atomic Force Microscopy and PM-IRRAS. *Biochim. Biophys. Acta, Biomembr.* **2010**, *1798*, 1503−1511.
(31) Aguayo, D.; González-Nilo, F. D.; Chipot, C. Insight into the Properties of Cardiolipin Bilayers from Molecular Dynamics Simulations, Using a Hybrid All-Atom/United Atom Force Field. *J. Chem. Theory Comput.* **2012**, *8*, 1765−1773.
(32) Niño, M. R. R.; Caro, A. L.; Patino, J. M. R. Structural, Topographical, and Rheological Characteristics of β-Casein-Dioleoyl Phosphatidylcholine (DOPC) Mixed Monolayers. *Colloids Surf., B* **2009**, *69*, 15−25.
(33) Broniatowski, M.; Flasiński, M.; Zięba, K.; Miśkowiec, P. Langmuir Monolayer Studies of the Interaction of Monoamphiphilic Pentacyclic Triterpenes With Anionic Mitochondrial and Bacterial Membrane Phospholipids — Searching for the Most Active Terpene. *Biochim. Biophys. Acta* **2014**, *1838*, 2460−2472.
(34) Gaines Jr., G. L. *Insoluble Monolayers at Liquid-Gas Interfaces*; Wiley: New York, 1966.
(35) Domènech, O.; Torrent-Burgués, J.; Merino, S.; Sanz, F.; Montero, M. T.; Hernández-Borrel, J. Surface Thermodynamics Study of Monolayers Formed with Heteroacid Phospholipids of Biological Interest. *Colloids Surf., B* **2005**, *41*, 233−238.
(36) Nichols-Smith, S.; Teh, S. Y.; Kuhl, T. L. Thermodynamic and Mechanical Properties of Model Mitochondrial Membranes. *Biochim. Biophys. Acta* **2004**, *1663*, 82−88.
(37) Aoki, P. H. B.; Volpati, D.; Caetano, W.; Constantino, C. J. L. Study of the Interaction Between Cardiolipin Bilayers and Methylene Blue in Polymer-Based Layer-by-Layer and Langmuir Films Applied as Membrane Mimetic Systems. *Vib. Spectrosc.* **2010**, *54*, 93−102.
(38) Zawisza, I.; Lachenwitzer, A.; Zamlynny, V.; Horswell, S. L.; Goddard, J. D.; Lipkowski, J. Electrochemical and Photon Polarization Modulation Infrared Reflection Absorption Spectroscopy Study of the Electric Field Driven Transformations of a Phospholipid Bilayer Supported at a Gold Electrode Surface. *Biophys. J.* **2003**, *85*, 4055−4075.
(39) Hasegawa, T.; Konk, V.; Leblanc, R. M. In *Vibrational Spectroscopy of Biological and Polymeric Materials*; Gregoriou, V. G., Braiman, M. S., Eds.; CRC Taylor & Francis Group: Boca Raton, FL, 2006; Chapter 3.
(40) Yu, Z.; Chuang, S. S. C. Probing Methylene Blue Photocatalytic Degradation by Adsorbed Ethanol with In Situ IR. *J. Phys. Chem. C* **2007**, *111*, 13813−1382.
(41) Vácha, R.; Jurkiewicz, P.; Petrov, M.; Berkowitz, M. L.; Bockmann, R. A.; Barucha-Kraszewska, J.; Hof, M.; Jungwirth, P. Mechanism of Interaction of Monovalent Ions with Phosphatidylcholine Lipid Membranes. *J. Phys. Chem. B* **2010**, *114*, 9504−9509.
(42) Christoforou, M.; Leontidis, E.; Brezesinski, G. Effects of Sodium Salts of Lyotropic Anions on Low-Temperature, Ordered Lipid Monolayers. *J. Phys. Chem. B* **2012**, *116*, 14602−14612.
(43) Barbosa, L. R. S.; Caetano, W.; Itri, R.; Homem-de-Mello, P.; Santiago, P. S.; Tabak, M. Interaction of Phenothiazine Compounds with Zwitterionic Lysophosphatidylcholine Micelles: Small Angle X-Ray Scattering, Electronic Absorption Spectroscopy, and Theoretical Calculations. *J. Phys. Chem. B* **2006**, *110*, 13086−13093.

DOI: 10.1021/acs.langmuir.5b00166
Langmuir 2015, 31, 4205−4212